Charge and mass distributions from the reaction of 240 MeV ^{12}C ions with ^{238}U

C. H. Lee and Y. W. Yu
College of Nuclear Science, National Tsing-Hua University, Hsinchu, Taiwan 30043, People's Republic of China

D. Lee, H. Kudo,* K. J. Moody,† and G. T. Seaborg
Lawrence Berkeley Laboratory, University of California, Berkeley, California 94720
(Received 12 January 1988; revised manuscript received 1 July 1988)

We have studied the reaction of 240 MeV ^{12}C ions with ^{238}U targets using radiochemistry techniques. We measured the formation cross sections of 139 radioactive nuclides. We have used these data to determine the charge and mass distribution of the fission products. The mass distribution is interpreted as a superposition of two main components: (1) products from high-energy fission processes, 3480±700 mb, and (2) products from low-energy fission, 1500±220 mb. We also estimate the production of targetlike nuclides to be 250±100 mb. The high-energy fission products can be resolved into products due to fusion-fission and fast fission, and products due to high-energy sequential fission. We have constructed the excitation functions of some product nuclides with $Z-Z_{pd}>2$.

I. INTRODUCTION

It is interesting to study the change in reaction mechanisms in heavy-ion-induced reactions as the incident projectile energy is varied, particularly at reaction energies near the nuclear Fermi energy. There is little published radiochemical work in this intermediate energy region. Most experiments performed at these energies have involved the measurement of the energy spectra of light emitted fragments.[1,2] In the reaction of ^{12}C ions with ^{238}U targets, radiochemistry studies have been performed at relativistic energies[3,4] and at energies near the Coulomb barrier.[5] At intermediate energies, the fission yields of Rb and Cs were measured with an isotope separator,[6] and the total fusionlike cross section was measured with position-sensitive multiwire detectors using the time-of-flight technique.[7] In a previous paper,[8] we found that the iodine isotope distribution can be fitted with the sum of two Gaussian curves. One component arises from the fission of precursors into which a substantial portion of the kinetic energy of the reaction has been damped (fast fission or sequential fission, depending upon the impact parameter). Most of these products do not arise from fusion-fission processes, since the average center-of-mass velocity of the fissioning system is only about a third of that expected for the compound nucleus. The other component is due to low-energy transfer-induced fission, where very little of the kinetic energy of the reaction is converted into center-of-mass motion of the fissioning system.

In this work, the charge and mass distributions of the products of the reaction of 240 MeV ^{12}C ions with ^{238}U are examined using radiochemical techniques. Measured mass distributions are decomposed into products due to high-energy fission, products due to low-energy fission, and targetlike products arising from transfer reactions. We have combined our data with data from the reaction of ^{12}C with ^{238}U at different energies, found in the literature, and have constructed excitation functions of the most neutron-deficient reaction products for incident projectile energies between 20 MeV/nucleon and 1000 MeV/ nucleon. Using these data we can try to understand the evolution of the reaction cross section from the Coulomb barrier to relativistic energies.

II. EXPERIMENT AND DATA REDUCTION

A. Cross-section determinations

Irradiations were performed with the 88-inch Cyclotron at the Lawrence Berkeley Laboratory. A 245 MeV $^{12}C^{5+}$ beam with an intensity of 20 electrical nanoamperes was delivered to the target foils, which were mounted at the back of an electron-suppressed Faraday cup. During the irradiations, the deposited charge was recorded periodically to permit the accurate reconstruction of the beam flux histories.

Each target stack consisted of a 27 mg/cm^2 depleted uranium foil sandwiched between two pairs of 6.24 mg/cm^2 aluminum foils with 99.99% purity. The uranium foil and the inner pair of catcher foils (containing forward- and backward-recoiling reaction products) were treated as a unit; the outer two foils served to protect the target stack against contamination by reaction products from the collimator and the beam stop. The upstream aluminum foils degraded the energy of the beam incident on the uranium foils to 240 MeV. The energy lost in the uranium itself was 12 MeV.[8]

Two irradiated targets were chemically separated into fractions containing alkaline earths, rare earths, halides, or actinide nuclides. In one run, the target stack was unprocessed. Gamma spectrometry was performed on the resultant samples with four Ge(Li) detectors operated in conjunction with 4096-channel analyzers. Gamma-ray spectra of each sample in the energy range between 50 keV and 2 MeV were taken as a function of time after the

TABLE I. Cross sections of individual radioactive nuclides produced in the interaction of 240 MeV ^{12}C ions with ^{238}U.

Nuclide	Measured yield (mb)	Type[b]	Independent yield (mb)	Mass yield (mb)
Sc 48	1.3±0.9	*C*		
Zn 69*m*	2.4±0.2	*I*	2.4±0.2	5.7±0.6[c]
Zn 71*m*	2.4±0.2	*I*	2.4±0.2	5.7±0.6[c]
Zn 72	2.8±0.4	*I*	2.8±0.4	10.5±1.4
Ga 72	5.2±0.5	*C*	5.2±0.5	
Ge 77*g*	3.3±2.0	*C*	2.9±1.8	10±6[c]
Ge 78	2.3±0.2	*C*	2.1±0.2	13.6±2.0
As 78	6.4±2.5	*C*	6.3±2.5	
Br 82	9.5±1.0	*I*	9.5±1.0	20.6±2.1
Kr 85*m*	7.4±1.0	*C*	6.1±0.8	[a]
Kr 87	10.2±1.0	*C*	8.2±0.8	30±4
Y 87	1.0±0.14	*C*	0.97±0.14	
Kr 88	6.7±0.7	*C*	5.4±0.5	27±4
Y 88	2.7±0.3	*C*	2.7±0.3	
Zr 89	0.8±0.2	*C*	0.78±0.19	39.5±9.6
Y 90*m*	9.7±1.0	*I*	9.7±1.0	[a]
Sr 91	29.6±3.0	*C*	16±2	66±10
Y 91*m*	18.0±2.9	*C*	14.8±2.4	
Sr 92	24.4±2.4	*C*	14±1	65±10
Y 92	24.1±2.4	*C*	18.4±1.8	
Y 93	38.0±3.8	*C*	24±2	94±9
Nb 95*g*	16.8±6.0	*C*	16.8±6.0	85±30[c]
Tc 95*g*	0.17±0.17	*C*	0.17±0.17	
Nb 96	14.5±5.9	*I*	14.5±5.9	81±23
Tc 96	2.5±0.6	*I*	2.5±0.6	
Zr 97	34.7±3.5	*C*	18.6±1.9	100±25
Ru 97	0.84±0.36	*C*	0.81±0.34	
Nb 98*b*	12.1±6.0	*C*	12.1±6.0	[a]
Mo 99	67.5±6.8	*C*	37.9±3.8	148±40
Tc 99*m*	1.6±0.2	*C*	1.6±0.2	
Ru 103	89.6±9.9	*C*	45±5	206±51
Ru 105	51.5±5.2	*C*	34±3	145±40
Rh 105	83.4±8.4	*C*	30±3	
Rh 106*m*	13.6±1.4	*I*	13.6±1.4	[a]
Rh 107	59.5±24.0	*C*	39±20	145±40
Pd 109	56.3±5.6	*C*	37±4	134±36
Pd 111*m*	5.1±0.5	*I*	5.1±0.5	89±9
Cd 111*m*	7.4±1.8	*I*	7.4±1.8	
In 111	1.4±0.1	*C*	1.34±0.13	
Pd 112	39.7±3.0	*C*	30±3	100±30
Ag 112	24.4±2.4	*C*	24.3±2.4	
Ag 113*g*	65.7±6.6	*C*	54±5	164±16[c]
Cd 115*g*	30.9±3.1	*C*	23.2±2.2	[a]
In 116*m*	22.5±14.7	*I*	22.5±14.7	[a]
Cd 117*m*	16.2±1.6	*C*	13.3±1.3	80±7
Cd 117*g*	6.0±0.6	*C*	4.9±0.5	
In 117*m*	22.5±14.6	*C*	22±14	
Sn 117*m*	16.7±3.5	*I*	16.7±3.5	
Sb 118*m*	5.3±0.6	*I*	5.3±0.6	[a]
Te 119*m*	1.9±0.3	*I*	1.9±0.3	[a]
Sb 120*b*	13.2±1.3	*I*	13.2±1.3	[a]
I 120*a*	0.34±0.03	*C*	0.31±0.12	[a]
I 121	2.0±0.9	*C*	1.9±0.9	103±50
Sb 122	25.2±2.5	*I*	25.2±2.5	70±7
I 123	12.2±2.1	*C*	12.2±2.1	103±14
I 124	17.7±2.6	*I*	17.7±2.6	93±9
Xe 125	4.7±0.5	*C*	4.4±0.4	65±7
Sb 126*g*	11.6±1.3	*I*	11.6±1.3	123±12

TABLE I. (*Continued*).

Nuclide	Measured yield (mb)	Type[b]	Independent yield (mb)	Mass yield (mb)
I 126	36.6±3.5	*I*	36.6±3.5	
Sn 127*g*	3.1±0.3	*C*	2.7±0.3	65±10
Sb 127	12.9±1.3	*C*	9.3±1.0	
Xe 127	12.4±1.6	*C*	10.2±1.3	
Cs 127	3.2±0.3	*C*	3.0±0.3	
Sn 128	5.6±1.0	*C*	4.6±0.8	77±20
Sb 128*g*	2.9±0.3	*C*	2.0±0.2	
I 128	23.3±7.1	*I*	23.3±7.1	
Ba 128	0.5±0.1	*C*	0.5±0.1	
Sb 129	6.1±0.6	*C*	5.4±0.5	75±25
Cs 129	16.8±1.7	*C*	14.5±1.4	
Sb 130*b*	4.8±4.8	*C*	3.9±3.9	101±20
I 130	14.5±2.8	*I*	14.5±2.8	
Te 131*m*	4.8±0.5	*C*	4.6±0.5	70±17
I 131	20.1±4.2	*C*	10.2±3.7	
Ba 131	6.9±0.7	*C*	6.9±0.7	
Te 132	14.7±1.5	*C*	12.0±1.2	79±15
I 132*m*	7.6±1.1	*I*	7.6±1.1	
I 132*g*	5.0±0.8	*C*	2.2±3.0	
La 132	2.7±0.3	*C*	2.1±0.3	
I 133	16.9±5.5	*C*	14.5±5.0	90±40
Xe 133*m*	5.9±3.8	*C*	5.9±3.8	
Xe 133*g*	9.9±3.5	*C*	2.6±3.1	
Ba 133*m*	18.0±1.7	*I*	18.0±1.7	
Ce 133*g*	0.43±0.07	*I*	0.43±0.07	
Te 134	13.3±3.1	*C*	10.8±2.5	104±35
I 134	15.8±5.5	*C*	12.6±4.4	
I 135	13.8±4.5	*C*	10.4±3.5	84±20
Ba 135*m*	17.6±1.7	*I*	17.6±1.7	
Ce 135	5.2±0.4	*C*	5.0±0.5	
Cs 136	6.9±0.7	*I*	6.9±0.7	55±6
Ce 137*m*	14.4±1.4	*I*	14.4±1.4	[a]
Pr 138*m*	5.3±0.5	*I*	5.3±0.5	[a]
Ba 139	16.5±2.2	*C*	10.8±1.4	79±10
Ce 139	31.1±2.9	*C*	21±2	
Nd 139*m*	2.4±0.8	*I*	2.4±0.8	
Ba 140	11.5±1.0	*C*	7.1±0.8	50±6
La 140	7.6±0.8	*C*	7.6±0.8	
La 141	9.8±2.0	*C*	6.1±1.2	66±15
Ce 141	36.2±5.4	*C*	18.3±1.8	
La 142	8.3±0.8	*C*	8.1±0.8	59±6
Pr 142	15.7±1.6	*I*	15.7±1.6	
Ce 143	12.6±1.3	*C*	7.9±0.8	57±6
Pm 144	8.8±0.9	*I*	8.8±0.9	52±18
Eu 145	0.32±0.07	*C*	0.32±0.07	41±9
Pm 146	8.8±3.0	*I*	8.8±3.0	46±6
Eu 146	1.0±0.1	*C*	1.0±0.1	
Nd 147	17.9±1.8	*C*	13.0±1.3	48±5
Eu 147	1.96±0.2	*C*	1.7±0.2	
Pm 148*m*	7.4±0.7	*I*	7.4±0.7	[a]
Nd 149	5.8±0.7	*C*	4.0±0.4	35±10
Pm 149	13.8±1.5	*C*	9.0±1.0	
Gd 149	1.5±0.1	*C*	1.4±0.1	
Pm 150	4.7±0.5	*I*	4.7±0.5	21±2
Pm 151	6.2±0.6	*C*	4.9±0.5	30±10
Gd 151	3.6±0.7	*C*	3.0±0.6	
Tb 151	0.91±0.14	*C*	0.87±0.13	
Sm 153	7.7±1.1	*C*	6.0±0.9	30±4
Eu 154	7.1±1.5	*I*	7.1±1.5	23±5

TABLE I. (*Continued*).

Nuclide	Measured yield (mb)	Type[b]	Independent yield (mb)	Mass yield (mb)
Tb 154*m*2	0.33±0.05	*I*	0.33±0.05	
Tb 154*m*1	2.6±0.3	*I*	2.6±0.3	
Tb 155	5.8±0.6	*C*	4.4±0.4	19±2
Dy 155	1.6±0.2	*C*	1.4±0.2	
Eu 156	4.0±0.4	*C*	3.7±0.4	20±4
Tb 156*m*	0.22±0.14	*I*	0.22±0.14	
Tb 156*g*	5.1±1.1	*I*	5.1±1.1	
Dy 157	4.2±0.4	*C*	3.7±0.4	17±2
Gd 159	1.2±0.2	*C*	1.1±0.2	9.4±1.7
Er 160	0.8±0.1	*C*	0.8±0.1	8.2±1.2
Tb 160	1.3±0.2	*I*	1.3±0.2	
Tm 165	2.2±0.2	*C*	1.9±0.2	6.9±0.7
Tm 166	1.9±0.2	*C*	1.8±0.2	6.0±1.0
Yb 166	1.1±0.3	*C*	1.0±0.3	
Tm 167	3.3±0.4	*C*	2.1±0.3	5.6±0.7
Yb 169	2.2±0.3	*C*	2.2±0.3	4.7±1.1
Lu 169	0.58±0.08	*C*	0.55±0.08	
Lu 171	1.24±0.14	*C*	1.22±0.14	3.9±0.4
Lu 172	0.83±0.08	*I*	0.83±0.08	2.2±0.2
U 237	90±30	*C*		90
Np 238	15±5	*I*		75
Np 239	10±5	*C*		35

[a]No mass yield was determined for this mass since only single members of isomeric species were observed.

[b]Measured independent yield (*I*), or cumulative or partially cumulative yield (*C*).

[c]The fission yield of the missing member of the isomeric pair was assumed to be negligible when the mass yield was calculated.

end of irradiation. The gamma-ray spectra were analyzed with a set of computer programs, described in detail in Ref. 9. Each gamma-ray peak in each spectrum was located, integrated and sorted into decay curves, which were interactively identified on the basis of gamma-ray energy and half-life. The initial activity of each nuclide was calculated from the extracted gamma-ray intensities and their absolute abundances.[10]

B. Calculation of charge and mass distributions

There are very few shielded nuclides for which we can directly determine the independent yield. Most of the independent yields are obtained from the measured partially cumulative and cumulative yields taking into account the decay of precursors. Since it is not possible to determine the yield of every nuclide needed for these corrections, it is necessary to use the systematic behavior of the independent yields as a function of product Z and A. This was accomplished with a modified MASSY program,[4] in which Gaussian charge dispersions are assumed:

$$\sigma(Z,A)=\sigma(A)[(2\pi S_Z^2)^{-1/2}\exp-(Z-Z_P)^2/\sqrt{2}S_Z^2]\ , \tag{1}$$

where $\sigma(A)$ is the isobaric yield, S_Z is the Gaussian width parameter, and Z_P is the most probable Z value of the charge dispersion curve at that value of A. As we noted in our previous work,[8] when two different reaction mechanisms contribute to the yield at a given mass, the sum of two Gaussian distributions with independent parameters can be used to fit the data.

Over a limited range, the Z_P values progress linearly with A for a given reaction mechanism. Since the width parameter and isobaric yield are slowly varying with the mass number, the experimental data of several neighboring mass numbers were pooled prior to fitting with a precursor distribution. The initial Gaussian parameters used to start the iterative process are chosen as follows: The Z_P and S_Z values for the most neutron-deficient products were calculated from the liquid-drop model, assuming formation of a compound nucleus.[11] The Z_P and S_Z values for more neutron-excessive products were assumed to be similar to those of the products from the interaction of 35 MeV protons with ^{238}U.[12]

III. RESULTS

A. Mass yields

Table I lists the 139 formation cross sections of radioactive nuclides which we determined in our experiments. The Z_P values resulting from the iterative correction of the cumulative yields for decay of precursors are given in Table II. The mass yield distribution deduced

TABLE II. Charge dispersion parameters in the reaction of 240 MeV ^{12}C ions with ^{238}U.

Mass range		Z_P	S_Z
69–82	(all)	$1.65+0.405\ A$	0.8
86–90	(n deficient)	$1.95+0.405\ A$	0.7
	(n excessive)	$5.5+0.35\ A$	0.7
91–109	(n deficient)	$1.95+0.405\ A$	1.0
	(n excessive)	$0.223+0.403\ A$	0.8
111–127	(n deficient)	$1.7+0.405\ A$	0.9
	(n excessive)	$-0.3+0.405\ A$	0.9
128–132	(n deficient)	$1.6\pm0.405\ A$	0.9
	(n excessive)	$19.2\pm0.25\ A$	1.0
133–143	(n deficient)	$1.7+0.405\ A$	0.9
	(n excessive)	$-4.5\pm0.43\ A$	1.0
144–157	(n deficient)	$1.29+0.405\ A$	1.1
	(n excessive)	$1.27+0.39\ A$	1.0
160–172	(all)	$1.0+0.45\ A-0.00026\ A^2$	1.0

from the experimental data is plotted in Fig. 1. The total yield between $A=60$ and $A=170$ is about 5710 mb and the total yield for targetlike products between $A=230$ and $A=240$ is estimated to be about 250 mb.

B. Charge dispersions

Table II gives the mass regions grouped together prior to extracting the independent yields with the MASSY program. The resultant Gaussian parameters are also given in Table II. Figure 2 shows the results of the fits plotted with the experimental data. It can be seen that only a single Gaussian component is necessary to explain the charge dispersion curves for mass regions from 69 to 82, and from 160 to 172. For the yields of nuclides with masses between 83 and 160, the data are fit with the sum of two overlapped Gaussians; the yields of the more neutron-deficient nucides arise from the sum of the fusion-fission process, the fast-fission process, and the sequential-fission process; the yields of the more

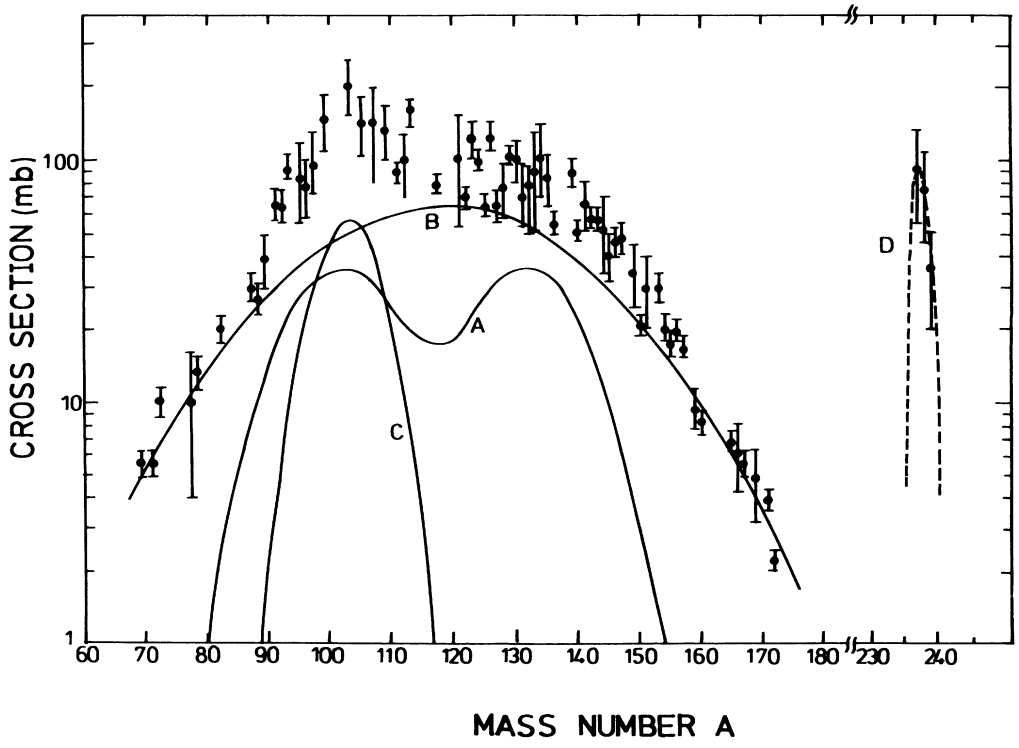

FIG. 1. Mass yield distributions measured in the interaction of 240 MeV ^{12}C ions with ^{238}U. The mass yields are decomposed into four components: (A) low-energy fission products, (B) products from the fusion-fission and fast-fission processes, (C) sequential-fission products, and (D) targetlike transfer products.

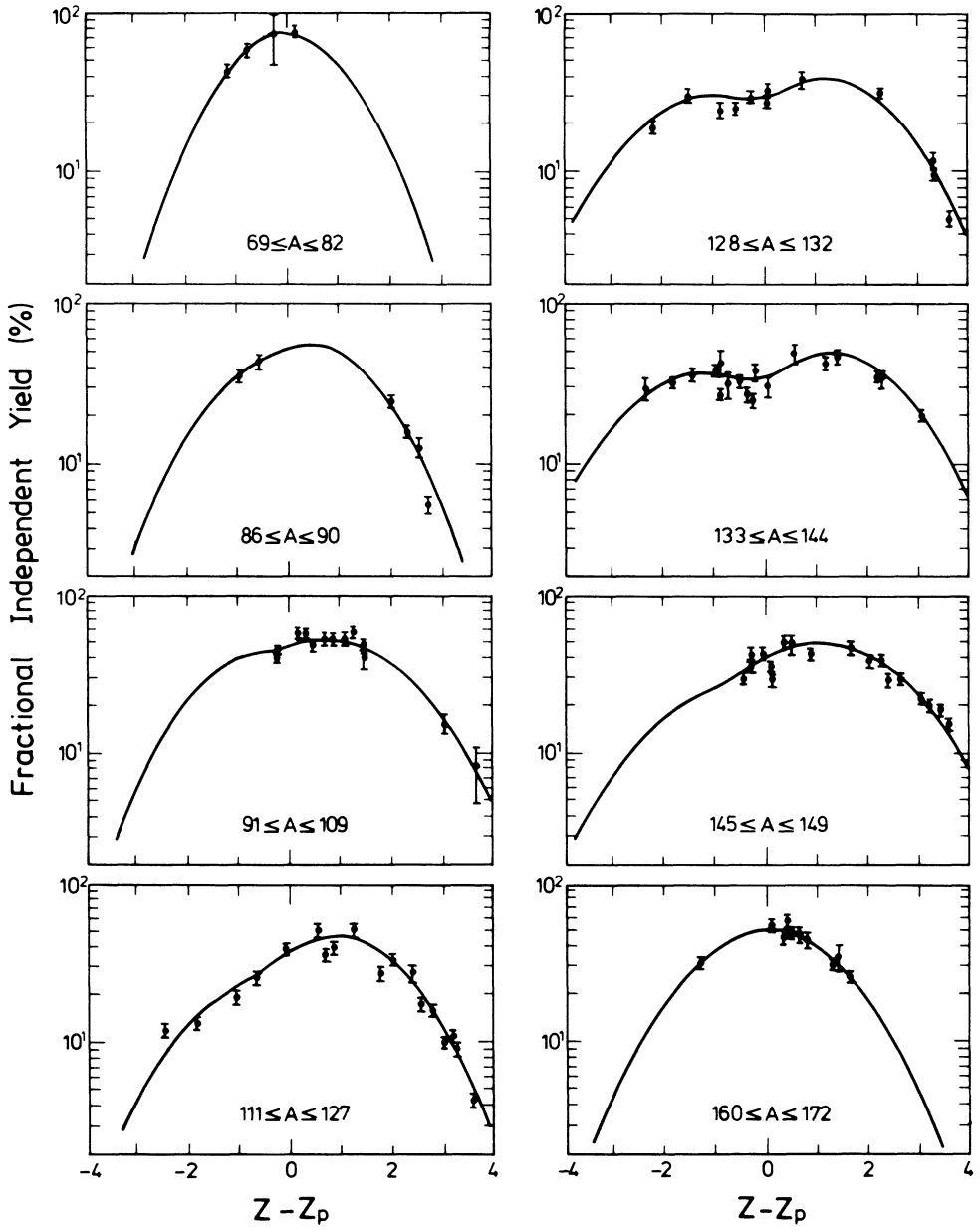

FIG. 2. Charge dispersions for several limited mass ranges of reaction products from the interaction of 240 MeV ^{12}C ions with ^{238}U.

TABLE III. Excitation functions of relatively neutron-deficient products of the reaction of ^{12}C ions with ^{238}U. Cross sections in mb. Data taken from Ref. 4 and this work.

Product	$Z-Z_P$	Projectile energy in MeV/nucleon 20	86	250	400	1000
Zr 89	2.31	0.8±0.2	5.7±0.6	9.3±0.5	12.9±1.1	13.8±1.3
Tc 96	2.17	2.5±0.6	3.9±0.4	5.8±0.4	6.4±0.6	6.5±0.8
In 111	2.10	1.4±0.1	5.0±0.7	8.2±0.5	9.7±0.9	10.1±0.7
Te 119	2.11	1.9±0.3	4.6±0.3	4.8±0.3	5.3±0.6	
I 121	2.30	1.9±0.9		10.0±2.4	9.1±1.3	13.0±2.0
Ba 128	2.56	0.5±0.1	2.3±0.6	4.3±0.5	4.4±1.2	4.7±0.5
Ce 133	2.44	0.43±0.01		4.0±0.7	4.2±0.4	4.0±0.9
Eu 145	2.985	0.32±0.07	2.3±0.2	8.2±0.4	9.5±0.7	9.3±0.8
Gd 149	2.365	1.5±0.1	2.3±0.4	8.2±0.6	7.5±1.1	9.4±0.9

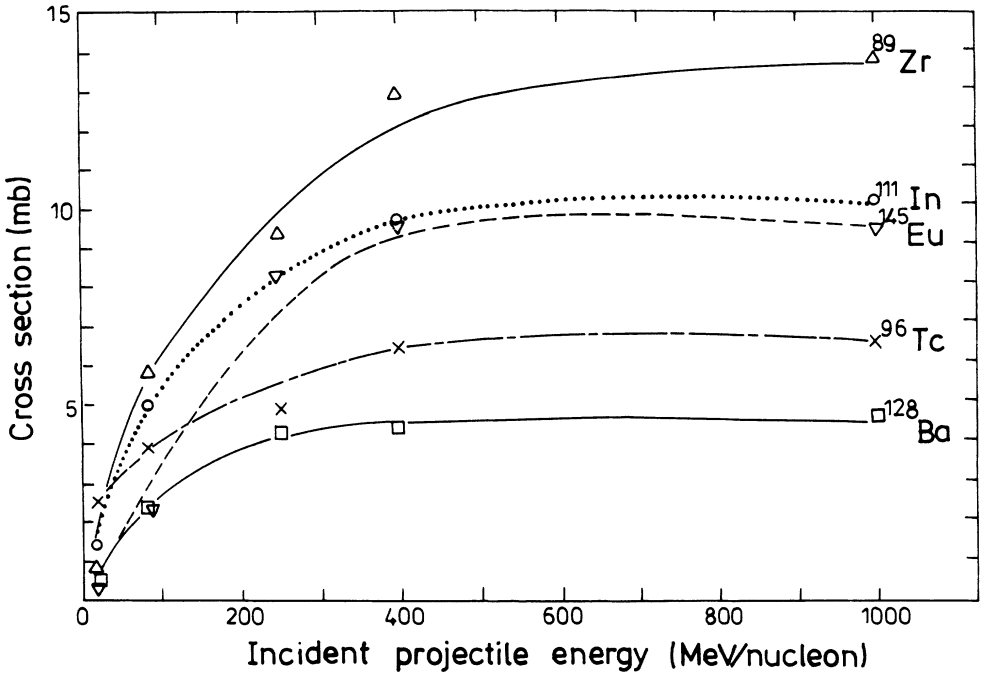

FIG. 3. Excitation functions of selected fission products from the reaction of ^{12}C and ^{238}U with $Z - Z_{Pd} > 2$.

neutron-excessive nuclides are formed from the combination of the low-excitation fission process (see Sec. IV A) and secondary reactions, which we estimate to contribute less than 10% of the neutron-rich yield.[8] Secondary components of the fit to mass regions from 86 to 90, from 91 to 109, and from 145 to 149 arise by requiring Gaussian widths compatible with the widths of the regions on either side. The fractional mass yields obtained by independently integrating the separate Gaussian components of the charge dispersion curves are approximately 4200 mb for the relatively neutron-deficient products and about 1500 mb for neutron-excessive products.

C. Excitation functions

To aid us in estimating the contributions to the high-energy processes, such as fast fission,[13] nonequilibrium fission processes, etc., the excitation functions of the relatively neutron-deficient products were constructed.

Table III lists some independent formation cross sections for nuclides with $Z - Z_{Pd}$ values greater than 2, at incident energies from 20 to 1000 MeV/nucleon. Z_{Pd} is the most probable charge of the more neutron-deficient Gaussian component. The excitation functions are plotted in Fig. 3. This shows that the yields of these products are sharply increasing with the incident projectile energy from 20 to 250 MeV/nucleon. For projectile energies above 300 MeV/nucleon, the excitation functions saturate.

IV. DISCUSSION

A. Fission yields

The measured mass yield distribution shown in Fig. 1 can be decomposed into the components indicated by the solid lines in the figure. The most neutron-excessive products are known to result from low-excitation fission processes,[8] such as few-nucleon-transfer-induced fission, Coulomb-induced fission, and fission resulting from secondary reactions. The charge distribution of the neutron-excessive Gaussian components, both in this work and in previous work,[8] was found to be very similar to the charge distribution of the products of the reaction of 35 MeV protons with ^{238}U in the mass region $A = 120-140$.[14] Therefore, we took the mass yield curve of the 35 MeV proton-induced products, from data in Ref. 15, and normalized it with the yield of the neutron-excessive Gaussians resulting from our work (1500 mb), and plotted it as the curve in Fig. 1 labeled A.

After subtraction of the low-energy fission products (component A) the remaining nuclides can be represented by two well-defined Gaussian distributions, labeled components B and C in Fig. 1. The center of component B is located at mass $A = 117.8 \pm 0.5$; the Gaussian has a full width at half maximum (FWHM) of 51.6 ± 0.6 mass units and a total area of 3480 mb. The center of component C is located at mass $A = 102.7 \pm 0.8$; the Gaussian has a FWHM of 11.8 ± 1.9 mass units and a total area of about 730 mb. All these relatively neutron-deficient products are formed from high-excitation nonperipheral collision

processes. Comparison of the FWHM, central location, and total yield of components B and C with products of ^{12}C-induced reactions at higher energies leads us to conclude that the yield of component B arises from a combination of the fusion-fission and fast-fission processes, and component C may arise from high-energy sequential-fission processes, in which substantial mass is lost from the targetlike product of the primary reaction prior to deexcitation by fission. These mechanisms will be discussed further in the following sections.

B. Yields from the fusion-fission and fast-fission processes

The mass distribution of the fission products is dominated by those nuclides arising from the fusion-fission and fast fission processes. Table IV lists the FWHM of the mass distributions of fission products from some reactions resulting in similar compound nuclei. All the values are similar to the FWHM of component B, except in the case of the interaction of 250 MeV ^{40}Ar ions with ^{209}Bi, where there is substantial production of "fission like" nuclides from damped collisions at large impact parameters.[16]

Since the fusion-fission and fast-fission processes lead to a symmetric mass distribution, the location of the center-of-mass distribution of these products, A_0, can be obtained with the expression:

$$A_0=(A_{CN}-\nu)/2\ , \tag{2}$$

TABLE IV. Full width at half maximum of the mass distribution of fission products of the reaction of various heavy ions with heavy target nuclides.

Reactions	Projectile energy (MeV)	FWHM (mass units)	Reference
$^{12}C+^{238}U$	105	43.3	5
$^{12}C+^{238}U$	113	45.6	5
$^{12}C+^{238}U$	122	49.1	5
$^{12}C+^{238}U$	240	51.6±0.6	This work[a]
$^{12}C+^{238}U$	1008	52	4
$^{18}O+^{232}Th$	102.5	49	21
$^{40}Ar+^{209}Bi$	215	55	16
$^{40}Ar+^{209}Bi$	250	70	16

[a]Includes only the sum of the fast-fission and fusion-fission components.

where A_{CN} is the mass of the compound nucleus ^{250}Cf, and ν is the total number of evaporated nucleons, most of which are neutrons. The value of ν can be obtained by comparison of the most probable charge values (Z_{Pd}) from Table II (plotted as solid line segments connecting the data points in Fig. 4) with the Z_{Pd} values calculated from equations given in Ref. 11. In these calculations, the mass and charge of the fission fragments can be related to the mass and charge of the fissioning system under the assumption of unchanged charge density (UCD)

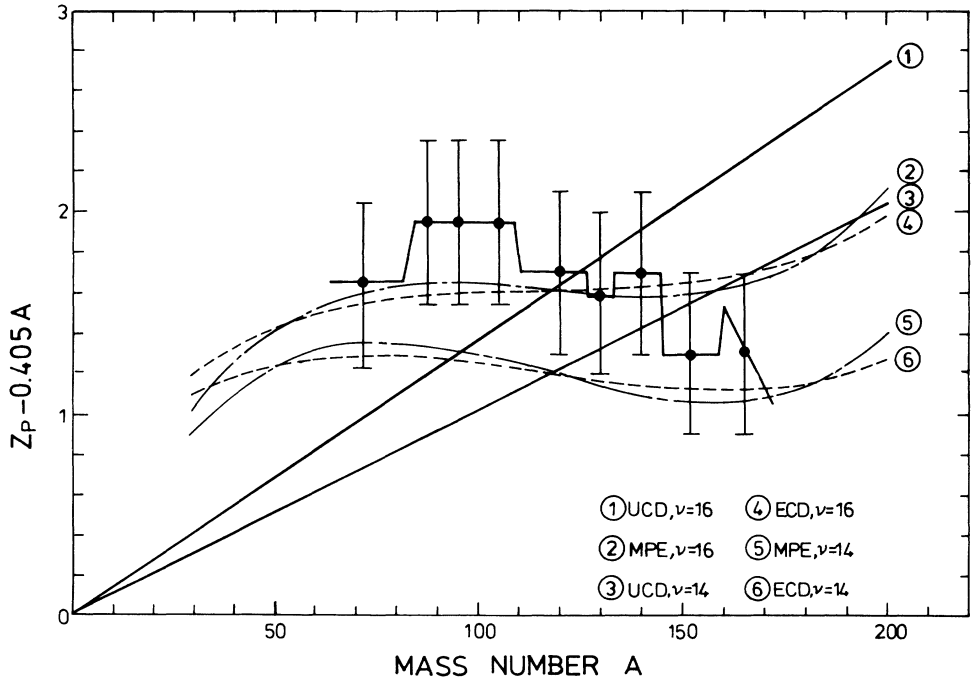

FIG. 4. Comparison of experimentally determined Z_P values for neutron deficient products of the reaction of 240 MeV ^{12}C ions with ^{238}U with those calculated from the liquid-drop model under several different assumptions. The error bars on the histogram data (from Table II) were obtained by the MASSY code from the statistical errors in the generation of the independent cross sections and from the spread of these values from the best functional fit to the data.

TABLE V. A comparison of the experimental "fusionlike" and total reaction cross sections from 240 MeV $^{12}C+^{238}U$ with calculated results from various models.

Source	Fusion cross section (mb)	Total reaction cross section (mb)	Ref.
This work	1740±350	3100±400	
Gavron *et al.* (experimental)	1900		7
Extra push model			17
$f=\frac{5}{7}$ (rolling)	1789		
$f=0.1827$ (sticking)	1855		
One-dimensional potential models			
Bass	1960		18
W. W. Wilke *et al.*	1054	3478	19
Critical distance model	1861		16
Empirical model of Gupta & Kailas		3259	20

(shown as straight lines in Fig. 4), equal charge displacement (ECD) (dashed curves in Fig. 4), or minimum potential energy (MPE) (dashed-dot curves). Continuous values of Z_{Pd} obtained with $\nu=14$ and $\nu=16$ are shown for each of the three assumptions. We find that the best fits to the experimental Z_{Pd} values are obtained with $\nu=16$ under all three postulates. From Eq. (2), the central location of the mass distribution of fission products arising from the fusion-fission and fast-fission processes is located at $A=117$, in agreement with the observed maximum of the component B Gaussian.

The "fusionlike" cross section obtained from component B (half the integrated fission product yield) is given in Table V together with calculations of this quantity arising from various models for the interaction of 240 MeV ^{12}C ions with ^{238}U. The extra push model[17] matches our experimental result both when the friction factor $f=\frac{5}{7}$ (rolling collision), and when $f=0.1827$ (sticking collision). The one-dimensional critical distance model[16] with the critical radius parameter $r=1.05$ fm also gives good agreement with our data. Similarly, the Bass model[18] yields a value very close to our measured result. The value arising from Wilcke's compilation,[19] which is more a measure of the true fusion cross section, is a factor of 2 lower than our combined fusion-fission plus fast-fission cross section. Our experimental data are also found to be in good agreement with the cross section of fusionlike nuclides measured by Gavron *et al.*[7]

This analysis, and the recoil properties of the relatively neutron-deficient iodine isotopes reported in our previous paper,[8] indicate that the reaction products of component B are formed from both the fusion-fission and the fast-fission processes. Using the component B cross section, we can extract an approximate limiting angular momentum for the two mechanisms of $82\hbar$, which is substantially larger than both $l_{cr}=64\hbar$, the limiting angular momentum for fusion of the $^{12}C+^{238}U$ system, and $l_{RLD}=70\hbar$, the angular momentum at which the liquid-drop fission barrier vanishes.[19] This indicates that the fast-fission process must contribute substantially to the cross section.

The total reaction cross section, obtained by summing half the areas of components A, B, and C, and the yields of targetlike products, is also given in Table V, along with calculated values from the works of various authors. It shows that our experimental value of 3100±400 mb is in good agreement with the value of 3259 mb calculated from Gupta and Kailas' empirical model[20] and the value of 3478 mb arising from one-dimensional potential models.[19]

C. Yields from high-energy processes

The reaction products of component C are relatively neutron deficient, similar to those of component B, but the center of the Gaussian distribution is located 14 mass units lower than that of component B. The FWHM of component C is much narrower. This information indicates that the component C products may be formed from the fission of precursor nuclides with mass numbers much less than that of both the compound nucleus and the target nuclide. This is probably due to a spallation-like process, where substantial mass is lost from the target nuclide prior to the fission step.

Since component C products arise from fission of the most neutron-deficient species, it might be expected that the contribution of the high-energy process is most important in the formation of the most neutron-deficient fission products. We see from the excitation functions in Fig. 3 that the yields of the most neutron-deficient reaction products are roughly a factor of 10 smaller than the yields of the same nuclides produced in reactions at relativistic energies, where only high-energy mechanisms contribute to the production of these nuclei. If we calculate the average ratio of the most neutron-deficient cross sections at 20 MeV/nucleon to those at higher projectile energies, and assume that this ratio holds for all nuclides produced from high-energy processes at 20 MeV/nucleon (which is only approximately true, at best), we can calculate a rough value for the contribution of high-energy processes to the reaction cross section at 20 MeV/nucleon. For 400 and 1000 MeV/nucleon ^{12}C interactions with ^{238}U, the total mass yields have been reported[4] to be 4000 mb in the mass region from $A=60-170$. Subtracting 1500 mb of fission yields attributed to the low-energy fission process, and taking 10% of the remainder, yields an estimate of 250 mb for the contribution of high-energy processes to the reaction cross section at 20 MeV/nucleon, which is only about a third of the observed yield of component C.

D. Yields of transfer reactions

We observed only three targetlike transfer reaction products, ^{237}U, ^{238}Np, and ^{239}Np. The mass yields are estimated utilizing the Gaussian widths reported in Ref. 11. The yield of U isotopes is about 180 mb and that of Np isotopes is 60 mb. If the yield of Pa isotopes is assumed to be 10 mb, the total yield for the targetlike products is 250 mb. Based on these approximations, we have estimated three mass yields, which are given in Table I.

E. A note on experimental uncertainties

The uncertainty in the cross section of each reaction component, obtained from the decomposition of the mass distribution curve of the reaction products, is estimated as follows: The yield from the low-energy fission process is based on the experimental mass distribution curve of the interaction 35 MeV protons with ^{238}U. Since the uncertainty in the experimental data is 10%, and a 10% error is assumed for the normalization of the peak height of the cross sections of neutron-excessive products, we use a total uncertainty of 15%, i.e., 1500±220 mb. The uncertainty of the yield arising from the sum of the fusion-fission and fast-fission processes is based on the error arising from the integration of the more neutron-deficient Gaussian from each charge dispersion curve; the total uncertainty for this process is about 20%, which gives a mass yield of 3480±700 mb. We do not know whether our assumption of using the yields of targetlike nuclides from the Ar+U reaction to fit charge dispersions to our data is entirely accurate, but we assume an error of 30% for this uncertainty, along with another 30% error arising from the errors on the cross sections of the individual data points, giving a result of 250±100 mb.

V. CONCLUSION

We have measured the formation cross sections of 139 nuclides produced in the interaction of 20 MeV/nucleon ^{12}C ions with ^{238}U. We have used this information to construct the charge and mass yield distribution curves, which we have deconvoluted into components to which we have attributed possible reaction mechanisms. The targetlike products, with a total cross section of 250±100 mb, are produced from transfer and secondary reactions. The fission products, with masses between 60 and 170, can be resolved into three different reaction components: (1) A broad distribution of relatively neutron-deficient products, which are produced from the fast-fission and fusion-fission processes, with a yield of 3480 mb. (2) A narrower distribution, also relatively neutron poor, centered at lower mass, which might be due to a high-energy sequential-fission process, with a yield of about 730 mb. (3) A "normal" neutron-excessive distribution, resembling the fission yield from the reaction of 35 MeV protons with ^{238}U, which is due to peripheral and secondary interactions, with a yield of 1500 mb. This yields a total reaction cross section of 3100 mb, in reasonable agreement with predictions.

ACKNOWLEDGMENTS

The authors would like to thank the members of the Heavy Elements group at the Lawrence Berkeley Laboratory for their assistance in performing the irradiations and the chemical separations. One of us (C.H.L.) is indebted to the Ministry of Education of the Republic of China for financial support. This work was supported by the Director, Office of High Energy and Nuclear Physics of the U.S. Department of Energy under Contract No. DE-AC03-76SF00098.

*Present address: Department of Chemistry, Faculty of Science, Niigata University, Niigata, Japan.

†Present address: Lawrence Livermore National Laboratory, L-232, P.O. Box 808, Livermore, CA 94550.

[1]B. B. Back, K. L. Wolf, A. C. Mignerey, C. K. Gelbke, T. C. Awes, H. Breuer, V. E. Viola, Jr., and P. Dyer, Phys. Rev. C **22**, 1927 (1980).

[2]D. K. Scott, Nucl. Phys. **A354**, 375 (1981).

[3]W. Loveland, C. Luo, P. L. McGaughey, D. J. Morrissey, and G. T. Seaborg, Phys. Rev. C **24**, 464 (1981).

[4]P. L. McGaughey, W. Loveland, D. J. Morrissey, K. Aleklett, and G. T. Seaborg, Phys. Rev. C **31**, 896 (1985).

[5]R. J. Otto, Ph. D. dissertation, Purdue University, 1972 (unpublished).

[6]M. de Saint Simon, S. Haan, G. Audi, A. Coc, M. Epherre, P. Guimbal, A. C. Mueller, C. Thibault, F. Touchard, and M. Langevin, Phys. Rev. C **26**, 2447 (1982).

[7]A. Gavron, J. Boissevain, H. C. Britt, K. Eskola, P. Eskola, M. M. Fowler, H. Ohm, J. B. Wilhelmy, T. C. Awes, R. L. Ferguson, F. E. Obenshain, F. Plasil, G. R. Young, and S. Wald, Phys. Rev. C **30**, 1550 (1984).

[8]Y. W. Yu, C. H. Lee, K. J. Moody, H. Kudo, D. Lee, and G. T. Seaborg, Phys. Rev. C **36**, 2396 (1987).

[9]D. J. Morrissey, D. Lee, R. J. Otto, and G. T. Seaborg, Nucl. Instrum. Methods **158**, 499 (1979).

[10]U. Reus and W. Westmeier, At. Data Nucl. Data Tables **29**, 1 (1983).

[11]J. V. Kratz, J. O. Liljenzin, A. E. Norris, and G. T. Seaborg, Phys. Rev. C **13**, 2347 (1976).

[12]C. Chung and J. J. Hogan, Phys. Rev. C **25**, 899 (1982).

[13]C. Gregoire, C. Ngo, and B. Remaud, Nucl. Phys. **A383**, 392 (1982).

[14]M. Diksic, D. K. McMillan, and L. Yaffe, J. Inorg. Nucl. Chem. **36**, 7 (1974).

[15]P. C. Stevenson, H. G. Hicks, W. E. Nervik, and D. R. Nethaway, Phys. Rev. **111**, 886 (1958).

[16]Z. Zheng, B. Borderie, D. Gardes, H. Gauvin, F. Hanappe, J. Peter, M. F. Rivet, B. Tamain, and A. Zaric, Nucl. Phys. **A422**, 447 (1984).

[17]J. R. Birkelund and J. R. Huizenga, Ann. Rev. Nucl. Part. Sci. **33**, 265 (1983).

[18]R. Bass, Nucl. Phys. **A231**, 45 (1974).

[19]W. W. Wilcke, J. R. Birkelund, H. J. Wollersheim, A. D. Hoover, J. R. Huizenga, W. U. Schroder, and L. E. Tubbs, At. Data Nucl. Data Tables **25**, 389 (1980).

[20]S. K. Gupta and S. Kailas, Z. Phys. A **317**, 75 (1984).

[21]R. L. Ferguson, F. Plasil, H. Freiesleben, C. E. Bemis, Jr., and H. W. Schmitt, Phys. Rev. C **8**, 1104 (1973).